

CIRCULAR ISOCENTRIC CONE-BEAM TRAJECTORIES FOR 3D IMAGE RECONSTRUCTIONS USING FDK ALGORITHM

D. Soimu, N. Pallikarakis

Department of Medical Physics, University of Patras, 26500 Patras, Greece

nipa@bme.med.upatras.gr

Abstract: Because of its highly computational efficiency and relative easy implementation, Feldkamp (FDK) reconstruction algorithm remains the most widely implemented method for 3D cone-beam (CB) reconstruction from x-ray projections, especially when the single circular isocentric orbit is used as source trajectory. For more complex trajectories (two orthogonal circles, circle-plus-arc, circle-and-line) usually exact reconstruction algorithms are used, but with the expense of computational requirements and implementation. The degree of inaccuracy of FDK reconstruction is highly object dependent, and the largest errors are to be expected for planes parallel to and remote from the midplane. In this study we used various circular isocentric acquisition setting trying to overcome this disadvantage. We compared the classical single-circular trajectory with the two-orthogonal and three-orthogonal circular trajectories. All projection acquired were used for object reconstruction using classical Feldkamp method, and considering the rotations of each trajectory plane from the standard one. Our results show that using two-orthogonal or three-orthogonal circular orbits, image quality of reconstructed slices greatly improves, and FDK algorithm can be used even for larger cone-angles.

Introduction

In the last years, there is an increasing interest on X-ray cone-beam (CB) tomography in medical applications, due to the properties of this approach: fast volume coverage, higher image resolution, easy hardware implementation, and lower radiation doses. Despite important progress in exact CB reconstruction algorithms [1, 2], the approximate methods remain practically important, and among them Feldkamp-type (FDK) formulas are the most popular [3]. The main advantages of this reconstruction algorithm are the possibility of using incomplete scanning loci, partial detection coverage, and especially their high computational efficiency.

The most common employed geometry for CB tomography is the circular isocentric orbit. From technical point of view, the circular scan path, in which the X-ray source rotates in a plane around the patient, is often the only feasible one, as alternate trajectories will involve patient's movement. But based on the single-circular source trajectory, mathematically exact reconstruction is possible only in the plane the source

rotates in. Increasing the distance from this central plane, CT image quality became more and more deteriorated. In general, the degree of inaccuracy in FDK reconstruction is highly object-dependent. As first pointed out by Feldkamp, the largest errors are to be expected for reconstructions plane parallel to and remote from the midplane. Another source of inaccuracy is represented by the cone-angle, which should be kept less than ten degrees (half). However, information could be added if additional circular concentric acquisition is used.

In this work, we compared the reconstructed images obtained from the classical single circular isocentric orbit, with the two- and three-orthogonal circular geometries for projection image acquisition in CBCT, using a FDK reconstruction method. Instead of one plane in which the source rotates, two or three isocentric orthogonal circular planes will be used. This type of acquisition setting can be used for head (brain), as well as for small animals/objects. The source may rotate in the two extra planes either completely (360°) or just for a limited angle, depending on the restriction imposed by the physical geometry and movement of the unit.

Materials and Methods

Due to its modest computational requirements and relative ease of implementation, FDK algorithm represents the most widely implemented method for 3D cone-beam reconstruction from transmitted x-ray projections. In the classical geometry scheme (single-circular), planar projections $P_\beta(p)$ of an object ($f(x,y,z)$) are obtained at a number of angles β . The reconstructed image is obtained by first convolving the weighted projection data with a filter kernel h , and then backprojecting the filtered data from every angle, according to the formula:

$$g(x,y) = \frac{1}{2} \int_0^{2\pi} \frac{d^2}{(d-s)^2} \int_{-\infty}^{\infty} P_\beta(p) * h\left(\frac{d}{d-s} - p\right) * \frac{d}{\sqrt{d^2 + p^2}} dp d\beta$$

where d is the distance from the source to the origin of the coordinate system, β is the rotational angle and $P_\beta(p)$ is the projection acquired at angle β .

Although this method is useful for many purposes, and is qualitatively informative, image reconstructed with this algorithm suffer from well known artifacts, arising from the approximate nature of the algorithm.

Reconstructed planes that are parallel and remote from the midplane are the ones that are mostly affected by these artifacts. To compensate for this effect, we used the two-orthogonal and three-orthogonal circular trajectories, so that every for every plane which is parallel to one of the circular trajectory we will have projection images taken from another non-parallel circular trajectory. The three-orthogonal consists of three circular orbits, so that the plane of one circle is perpendicular on the other two planes. For simplicity of computations, all orthogonal orbits are supposed to be concentric and have the same radius (figure 1).

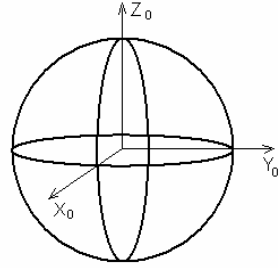


Figure 1: Geometry for three-orthogonal circular isocentric orbit.

The reconstruction formula is the same like above, but we take into account the rotation of acquired projections with respect to the classical settings: considering that the classical circular trajectory is around Y_0 -axis, that is the rotation plane is (X_0, Z_0) , the others two source rotation planes for this geometry will be (Y_0, Z_0) and (X_0, Y_0) . The Euler angles between the first rotation plane and the second one are $(\Phi = 0^\circ, \Theta = -90^\circ, \Psi = -90^\circ)$, and $(\Phi = 90^\circ, \Theta = 90^\circ, \Psi = 0^\circ)$ between first and third rotation plane. The source can rotate completely in every plane, or just over a limited arc, depending on imaged objects and system particularities.

For this study noise-free projection of two simulated phantoms were used: The Kudo-Defrise phantom, (seven ellipsoid disks) and the head (Shepp and Logan) phantom were simulated using the Simphan software data generator for radiographic imaging investigations [4, 5]. This in-house investigative tool software can be used to simulate the entire radiological process, including the imaged object, imaging modalities, operating parameters, beam transport. It provides sufficient accuracy and flexibility to allow its use in a wide range of approaches, been of particular help in the design of an experiment and the conduct of first level trials [5]. We used simulated data because it is particularly useful in studying specific effects, being free of distortions and others inaccuracies inherent to radiographic units [6]. For real data, preprocessing of projection images is needed prior to reconstruction in order to correct for pincushion distortion and errors due to earth magnetic field [7], but also for system inhomogeneities and sampling errors [8].

The ellipsoids phantom has been widely used to evaluate the performance of analytic cone-beam reconstruction algorithms, because it can effectively

demonstrate the artifacts caused by incompleteness of projections when using the single-circular cone-beam geometry. Our simulated phantom consists of seven ellipsoids of equal size, separated by a distance of 30 mm along the Y_0 axis. The lengths of the semi-major axis of ellipsoids are 100, 7.5 and 100 mm in the x, y, and z direction respectively. The density of the objects is assumed to be 1 inside the ellipsoids and 0 outside.

Because the two- and three-orthogonal geometry can be used with minimal requirements for the head, a three-dimensional version of Shepp-and-Logan head phantom was also simulated. This phantom consists of 12 ellipsoids with a very tight range of absorption coefficients, and was used to test the accuracy of the algorithm of reconstructing cross-sections of the human head.

Projection images of these two phantoms were generated considering an isocentric rotation over 360° in each trajectory, at an angular step of 4° . Two sets of projection were acquired for each phantom and each geometry orbit, first for a cone angle of 10° , and the second for a 24° cone-angle. In the numerical simulations, for both phantoms we used a 36.5 by 36.5 cm detector, with 256 by 256 pixels (image resolution = 7 pixels/cm). The source-to-isocenter (SID) distance was 100cm, and source-to-image intensifier (SIID) distance 130cm for the 10° cone-angle, while for the 24° cone-angle settings SID = 50cm and SIID = 65 cm.

In order to verify the performance of Feldkamp algorithm for the different orbits used, the *Root Mean Square (RMS) error* was computed for all the reconstructed images, as an objective image characteristic, using the following formula:

$$RMS.error = \frac{1}{I * J * K} \sqrt{\sum_{i=1}^I \sum_{j=1}^J \sum_{k=1}^K (f_{ijk} - f_{ijk}^t)^2} ,$$

where $f_{i,j,k}$ is the reconstructed 3D image(volume) with dimensions I, J, K and f_{ijk}^t is the ideal (theoretical) value of the image. Moreover, profiles along central horizontal line were plotted to underline the differences between Feldkamp algorithm applied to classical single-circular geometry and the two- and three- orthogonal geometries.

Results

The simulation results are shown in figures 2-5. Figure 2 shows the central sagittal/vertical reconstructed slice of the Kudo-Defrise phantom, for cone-angles of 10° (1) and 24° (2), when projections where acquired with single (a), two- (b) and three-orthogonal (c) circular orbits. The source rotates completely over 360° in all acquisition settings. It is easily observed that for larger cone angle the two- and three-orthogonal circular trajectories continue to result in well-defined objects (b2, c2), although some reconstruction blurring is introduced.

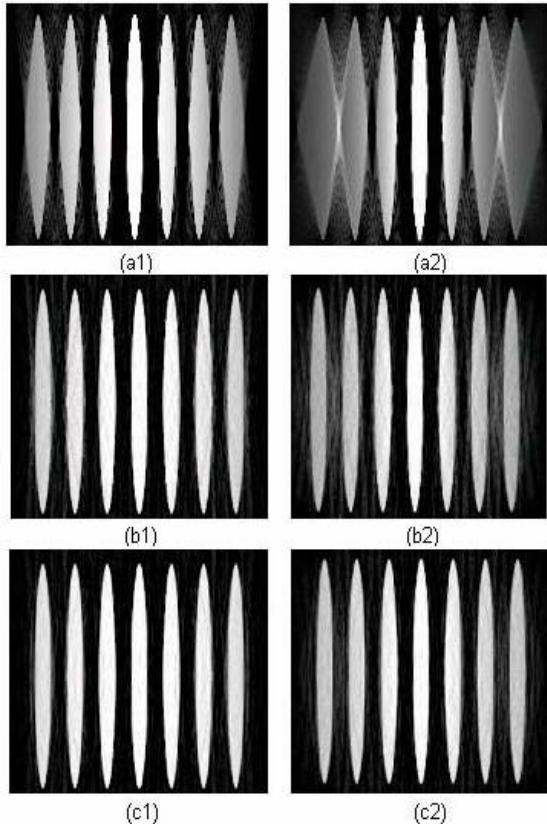


Figure 2: The central sagittal slice of the ellipsoids phantom, using 10° (a1, b1, c1) and 24° (a2, b2, c2) cone-angle and the single (a), two (b) and three-orthogonal (c) circular trajectories.

The line-profile corresponding to each image of figure 2, is shown in figure 3. The comparison of these images and their corresponding profiles, shows that with the use of the large cone-angle (24°), the FDK algorithm based on projection images acquired from a single circular orbit, introduces severe artefacts when reconstructing planes that are perpendicular to the midplane. The others two setting hold up reasonable well even for larger cone-angle: flat objects remote from centre are still well defined; the edges are conserved, although some blurring is introduced. The windowing range for all ellipsoid-phantom images is [0.3 - 1.0].

Figure 4 presents the RMS errors plots for axial planes (planes that are parallel to the midplane in the initial setting acquisition) for both 10° and 24° cone-angles. In this case the ellipsoids were reconstructed at distances: -3 cm, 0 cm, 3 cm and 6 cm from midplane. It is again obvious that the two- and especially the three-orthogonal setting, performs better (in terms of RMS errors) with reconstruction planes parallel to and remote from midplane for larger cone angles. In figure 5, reconstructed sagittal slices of Shepp-Logan phantom at $z = -2.5$ cm for a cone-angle of 24° are shown. Images reconstructed with two and three-orthogonal geometry show again a better reconstruction quality. The display

scale for these images has been concentrated in the density range [0.95- 1.05] for clarity.

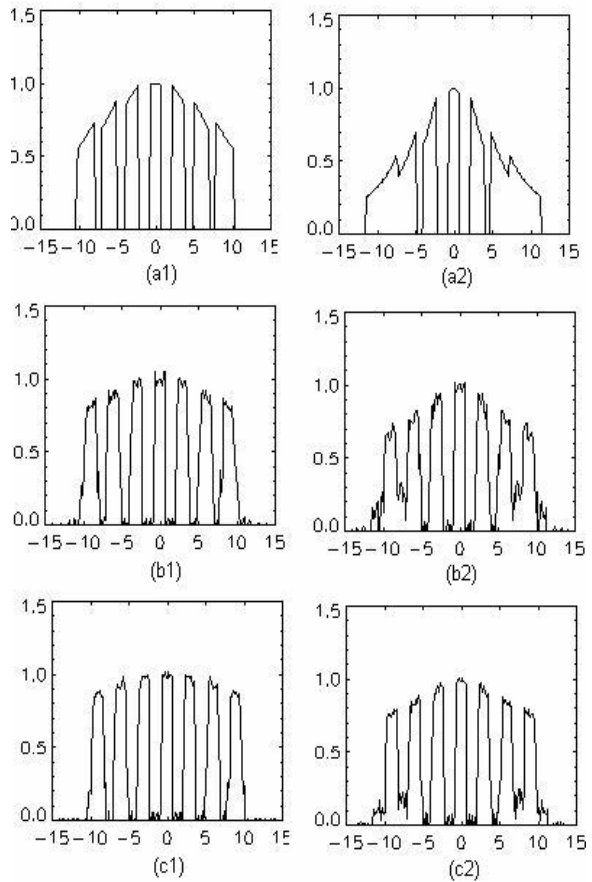


Figure 3: Profiles along the central horizontal lines of the images in figure 1: (a1) and (a2) for single circular orbit for 10° and 24° respectively, (b1) and (b2) for two-orthogonal orbit and (c1), (c2) for the three orthogonal geometry.

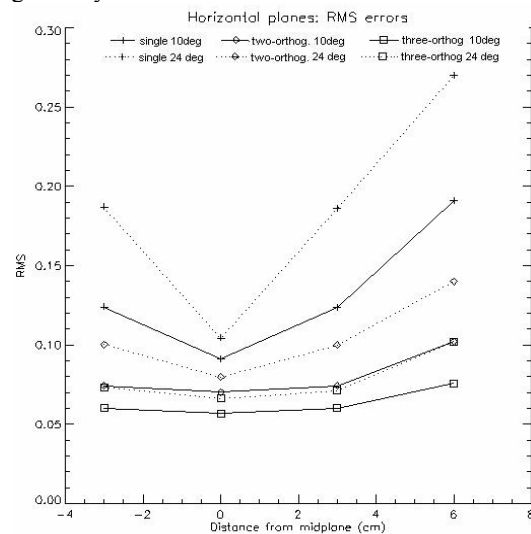


Figure 4: Root Mean Square (RMS) reconstruction errors for single, two- and three-orthogonal circular orbits.

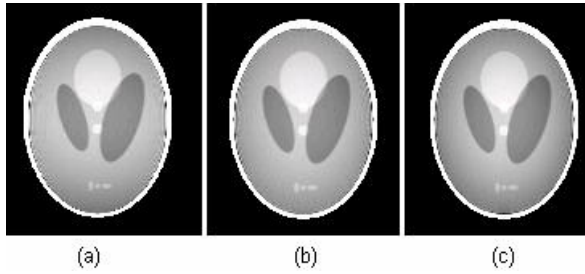


Figure 5: Reconstructed image of Shepp-Logan phantom using single-circular (a), two-orthogonal (b) and three-orthogonal (c) orbits at cone-angle of 24° .

The simulated projections were acquired with the in-house Simphan Simulator, and the reconstructions were performed on a Celeron 366MHz computer, using IDL language. It took about 42 seconds to reconstruct an image plane of 256^2 pixels if the single circular orbit was used, and about 100 seconds to reconstruct the same image with the three-orthogonal circular isocentric geometry.

Discussion

As seen from the above figures, using two- or three-orthogonal orbit for data acquisition, provides better results for 3D image reconstruction, both in terms of RMS error (figure 4) and artifacts (figures 2, 3, 5).

Using FDK reconstruction with the singular circular trajectory, greater errors are expected for a flat object parallel to and far from the midplane. This is obvious from figure 4, where reconstruction of similar ellipsoids at distance -3, 3 and 6 cm from midplane, show increasing of RMS errors. Reconstruction of such an object is smeared in the vertical direction; smearing is increasing with increasing object distance from the midplane, due to the fact that the shadow of the outer portion of the object results in an apparent reduced density below and above the object. Using the two or three orthogonal orbit will reduce this effect.

The large cone-angle problem can also benefit by using these trajectories. While for a cone-angle of 24° , the FDK reconstruction from the single-circular orbit data introduces severe artifacts (figures 2, 3), the quality of the same reconstructed slice from projection acquired with the other two geometries improves significantly, though some reconstruction noise (blurring) is added. Especially the three-orthogonal setting perform reasonable well for larger cone-angles, the errors for reconstructed planes remote from midplane being significantly reduced (figure 4), and the edges and abrupt density changes are better conserved.

The scan method for two- and three-orthogonal geometry can be implemented with minimal requirements, and without introducing much mechanical complexity. It can be used for the head and also for research purposes involving small animals/objects with a diameter of 25-35 cm, which require a larger cone-angle for image acquisition.

Conclusion

The Feldkamp 3D cone-beam reconstruction from projection data acquired along a single circular source-detector trajectory is a computationally efficient, and gives good results if some conditions are met. Using projections obtained from more than just one circular orbit, some of the artifacts, due to FDK approximate nature, are reduced (the large cone-angle problem, the blurring of slices parallel to and far from the midplane), while keeping the advantages that made this method so popular: easy implementation and fast computational time.

References

- [1] SMITH B. D. (1985): 'Image reconstruction from cone-beam projections: necessary and sufficient condition and reconstruction method', *IEEE Trans. Med. Imaging*, **4**, 14-28
- [2] GRANGEAT P. (1991): 'Mathematical frameworks of cone-beam 3D reconstructions via the first derivative of the Radon transform', in HERMAN, LOUIS, NATTERER (Ed): 'Lectures notes in Mathematics', (Springer-Verlag, Berlin), pp. 66-97
- [3] FELDKAMP L. A., DAVIS L. C., KRESS J. W. (1984): 'Practical cone-beam algorithm', *J. Opt. Soc. Am.* **A1**, 612-619
- [4] LAZOS D., KOLITSI Z., PALLIKARAKIS N. (2000): 'A software data generator for radiographic imaging investigations', *IEEE Trans. Inf. Biomed.* **4**, 76-79
- [5] BLIZNAKOVA K (2003): 'Study and development of software simulation for X-ray imaging', PhD thesis (Patras University, Greece)
- [6] BADEA C. (2000): 'Volume imaging using a combined Cone Beam CT - DTS Approach', PhD. thesis (Patras University, Greece)
- [7]. SOIMU D., BADEA C., PALLIKARAKIS N. (2003): 'A novel approach for distortion correction for X-ray image intensifiers', *Comput. Med. Imaging Graph.* **27(1)**, 79-85
- [8] BADEA C., KOLITSI Z., PALLIKARAKIS N. (2001): 'Image quality in extended arc filtered digital tomosynthesis', *Acta Radiologica*, **42**, 244-249